Pairing space-charge field conditions with self-guiding for the attainment of circular symmetry in photorefractive solitons

E. DelRe
Dipartimento di Fisica, Universita' dell'Aquila, 67010 L'Aquila, Italy and Istituto Nazionale Fisica della Materia, Unita' di Roma "La Sapienza," 00185 Rome, Italy

G. De Masi and A. Ciattoni
Dipartimento di Fisica, Universita' dell'Aquila, 67010 L'Aquila, Italy and Istituto Nazionale Fisica della Materia, Unita' dell'Aquila, 67010 L'Aquila, Italy

E. Palange[a)]
Dipartimento di Ingegneria Elettrica, Universita' dell'Aquila, 67040 Monteluco di Roio (L'Aquila), Italy and Istituto Nazionale Fisica della Materia, Unita' dell'Aquila, 67010 L'Aquila, Italy

(Received 4 August 2004; accepted 9 October 2004)

By means of a comparative study, we identify a specific physical mechanism that leads to circular-symmetric two-dimensional photorefractive solitons, and determine the conditions for their observation. For a given photorefractive crystal, this allows the control of the transition from an elliptical soliton-supporting regime to a round soliton-supporting one. This indicates a basic recipe to generate electro-optic devices in three-dimensional crystals compatible with single-mode fiber. © *2004 American Institute of Physics*. [DOI: 10.1063/1.1830075]

Photorefraction supports optical spatial solitons both in one and two transverse dimensions.[1] The two-dimensional (2D) realization forms a fundamental component to a family of innovative optical techniques, which range from optically written components,[2] electro-optically reconfigurable interconnects,[3] to the enhancement of second-order (χ^2) response.[4] The underlying nonlinearity is generally anisotropic and solitons reflect this in a generally elliptic intensity profile I. In some cases, the nonspreading beam has a bell-shaped circular-symmetric (round) intensity distribution, and this condition arouses particular physical and applicative interest.[5] Since round propagation modes characterize both the more general class of saturated solitons and standard optical components, such as single-mode fiber, a round photorefractive soliton forms a natural extension of single-mode guided circuits into three-dimensional electro-optic material.[6] In this regard, the absence of a clear understanding of the mechanisms that control this transverse beam shape represents a basic obstacle.[7,8] This can be attributed to the complexity of the photorefractive 2D nonlinearity, which on top of being anisotropic, is also nonlocal,[8–11] with sample-dependent characteristics.[12] The end result is that devices based on 2D solitons can be difficult to design and reproduce.

The issue is well illustrated by the apparent incompatibility of experiments that find *round* self-trapping for a set of parameters,[5,7,13–15] and a second family of observations that find *only elliptic* self-trapping.[8,12,16,17] The first suggest that the nonlinearity can be approximated by a local saturated response,[18] but this is at odds with the fundamentally anisotropic nature of the self-lensing.[11,19,20] A possible unified picture based on pulsing along the propagation axis[8] is excluded by dedicated studies.[7] A step forward has been achieved by also considering effects due to charge diffusion and saturation, neglected in these early 2D approaches.[9] Although the effort allows only numerical predictions, these include *both* round and elliptical self-trapping.

The present effort is thus aimed at formulating a hypothesis for the underlying physical mechanism leading to round soliton formation, predicting the associated conditions, and carrying out an experimental verification.

Given the complexity of the mechanisms involved, our approach is based on a comparative study. The rationale is to experimentally find and investigate two conditions that would be physically identical in a local isotropic model, but that lead to qualitatively distinct self-trapping phenomena: in one, round solitons form, whereas in the other, no accessible system parameters allow for the symmetric manifestation. The discriminating mechanism is then identified through the analysis of the observed differences in the underlying nonlinear response through electro-optic readout.[21] In order to exclude material-dependent effects, the study is realized in the *same* sample.

Since diffusion and saturation components are the key to the process,[9] and they depend on the transverse spatial scale, by using different input beam sizes $\ell_0=\Delta x_0=\Delta y_0$, we proceed through a set of experiments in which their relative weight, compared to the anisotropic response, is changed. Monitoring the output soliton full width at half-maximum of the intensity distribution, along the two transverse axes $(\Delta x,\Delta y)$ and the corresponding round self-trapping size $\ell=\Delta x=\Delta y$, we analyze the relationship between shape and size in the steady-state regime.

The setup, described in Refs. 1 and 14, makes use of a zero-cut $3.7^x\times 4.1^y\times 2.4^z$ mm crystal of paraelectric potassium lithium tantalate niobate (KLTN), with a temperature-dependent dielectric constant $\epsilon_r(T)$. The Gaussian launch beam was obtained from a cw x-polarized argon-ion laser operating at $\lambda=514$ nm. The input beam size ℓ_0 was controlled by the focusing optics. Steady-state was attained by launching a copropagating y-polarized plane wave of intensity I_b, and applying an external constant bias field E_0 along the transverse x-axis. For each experiment, the input inten-

a)Electronic mail: palange@ing.univaq.it

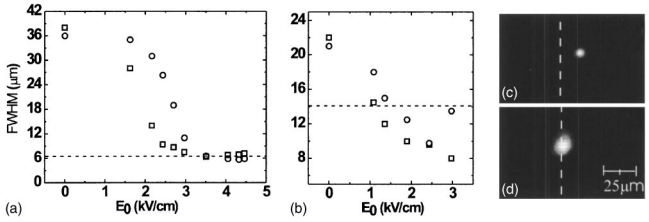

FIG. 1. Approach to round self-trapping in the two regimes. Δx (squares) and Δy (circles) vs E_0 for (a) $\ell_0=6.5\ \mu\mathrm{m}=\ell$ and (b) $\ell_0=14\ \mu\mathrm{m}\neq\ell=10\ \mu\mathrm{m}$. Horizontal lines indicate ℓ_0. Output intensity distribution for $\Delta x=\ell_0$ in the two regimes: (c) a circular soliton with a 18 μm shift and (d) an elliptical shape with a 2 μm shift. Vertical line indicates input x position.

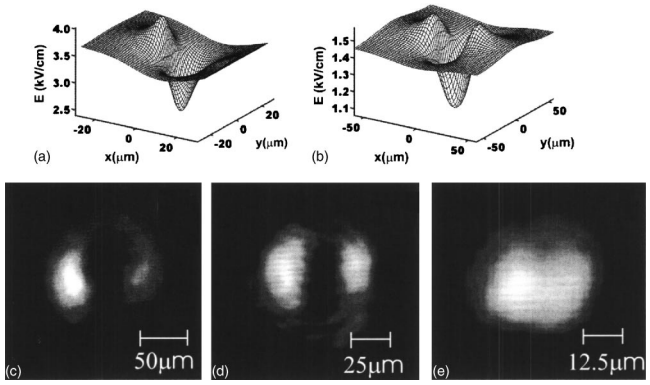

FIG. 2. Lobe suppression. Numerical calculation of the x-component of the space-charge field neglecting propagation effects, for (a) $\ell_0=6.5\ \mu\mathrm{m}$ and (b) $\ell_0=14\ \mu\mathrm{m}$. Observed output intensity distribution with a zero-field readout (Ref. 21), for (c) $\ell_0=6.5\ \mu\mathrm{m}$, (d) 11 μm, and (e) 14 μm, in conditions in which $\Delta x=\ell_0$.

sity ratio was fixed to a given $u_0^2=I_p/I_b$, where I_p is the peak beam intensity.

We identified two qualitatively different situations for $\ell_0\simeq 6.5$ and 14 μm, shown in Fig. 1, and these constitute the extremities of our comparative study. For $\ell_0=6.5\ \mu\mathrm{m}$, we scan different values of launch u_0 and different values of bias field E_0. As shown in Fig. 1(a), for $u_0\simeq 2.4$ and $\epsilon_r\simeq 12\,500$, a value of $E_0\simeq 3.5$ kV/cm traps the beam to a round $\Delta x=\Delta y=\ell\simeq 6.5\ \mu\mathrm{m}$ soliton, accompanied by an 18 μm bending shift for a longitudinal propagation of 2.4 mm Fig. 1(c). A different situation is found in the second case of Fig. 1(b), where the beam launched with a waist of $\ell_0\simeq 14\ \mu\mathrm{m}$ does not converge to a round soliton of $\ell\simeq\ell_0$ for *any* values of E_0 and u_0. The reported scan in E_0 refers to a launch $u_0\simeq 1.4$ and $\epsilon_r\simeq 11\,000$, and corresponds to the condition in which self-trapping manifests the lowest beam ellipticity (scanning both lower and *higher* values of u_0). We can compare the two scans directly by observing the situation in which $\Delta x\simeq\ell_0$ Figs. 1(c) and 1(d). In the second case, the beam ellipticity is $\Delta y/\Delta x\simeq 1.3$ and the associated bending shift is of 2 μm Fig. 1(d). As also shown in Fig. 1(b), increasing E_0 leads to a decrease in Δx and Δy, and, eventually, for $\ell\simeq 9.5\ \mu\mathrm{m}$, to the formation of a *round* soliton. Scans for intermediate values of $\ell_0\simeq 8$ and 11 μm, indicated a continuous transition from one regime to the other, the first allowing for a round soliton at $\ell\simeq\ell_0$, the second only at the condition of having ℓ slightly lower than ℓ_0.

The existence of these distinct regimes, dictated by the spatial scale ℓ_0, is in contrast with standard self-trapping phenomena, in which the local isotropic model leads to only one relevant physical quantity, $\Delta\xi=\ell_0/d$,[1] as a function of u_0. Here, $d=(2k^2\Delta n_0/n)^{-1/2}$ is the nonlinear spatial scale determined by E_0 through the electro-optic response $\Delta n_0=(1/2)n^3 g\epsilon_0^2(\epsilon_r-1)^2E_0^2$, where $k=2\pi n/\lambda, n\simeq 2.3$ is the unperturbed index of refraction, and $g\simeq 0.13\ \mathrm{m}^4\ \mathrm{C}^{-2}$ is the quadratic electro-optic coefficient.

Pursuing the logic of our comparative approach, we analyze the details of the photorefractive/electrostatic 2D problem,[1] in the two cases of Figs. 1(c) and 1(d). The corresponding numerical calculation of the x-component of the space-charge field $E(x,y)$ in the two conditions, which translates into the index pattern $\Delta n(x,y)$ through the electro-optic effect, is shown in Figs. 2(a) and 2(b). The striking feature is that the strongly distorted case of Fig. 2(a) leads to a round soliton, whereas the x-symmetric case of Fig. 2(b) leads to an elliptical beam shape. We deduce that in the first case, the smaller $\ell_0=6.5\ \mu\mathrm{m}$ activates a relevant nonlocal (asymmetric) component due to charge diffusion and saturation, which at once tilts the index pattern and suppresses one of the two lateral lobes. The process is negligible in the second case, for which the larger value of $\ell_0=14\ \mu\mathrm{m}$ leads to smaller nonlocal components. We tested this phenomenological conjecture experimentally, through the readout, at zero bias field, of previously imprinted index patterns for different spatial scales.[21] The $\ell_0=6.5$, 11, and 14 μm readouts are shown in Figs. 2(c)–2(e), respectively. As expected, the first readout shows an asymmetric lobe structure and leads to a round soliton. The other two (the 11 μm case being intermediate), have an increasing symmetry in the lobes, not allowing the formation of round solitons. This brings us to formulate the hypothesis that the lensing in the x-direction, generally stronger than in the y-direction, is weakenod by the suppression of one of the lobes. The resulting asymmetry due to the enhancement of the remaining lobe causes soliton bending (self-refraction), without appreciably affecting the transverse shape.

This picture implies *two* independent conditions: that (i) the resulting index pattern support the soliton; and (ii) one of the lobes be suppressed. Condition (i) is equivalent to verifying that the parameters (E_0,u_0,ℓ) giving rise to the soliton-supporting refractive index pattern Δn, compensate diffraction. This condition can be estimated neglecting all nonlocal and anisotropic effects (for example, see Fig. 3 in Ref. 10).

Condition (ii) implies that, in the region manifesting the lobes, the configuration leading to round solitons must be associated with a given precise relationship between the nonlocal x-component of the space-charge field response, $E_n=E_d+E_s$ (due to the diffusion component E_d and charge saturation one E_s), and the corresponding anisotropic part E_a (the lobes). This relationship must be preserved for all conditions leading to round solitons, for different parameters (E_0,u_0,ℓ), implying a condition on their scaling that we can experimentally test. An estimate of the diffusion and saturation field, for example, along the lines of the approximate approach of Ref. 22, indicates, respectively, that $E_d\propto(k_\mathrm{B}T/q)u_0^2(1+u_0^2)^{-1}\ell^{-1}$ and $E_s\propto\epsilon_0\epsilon_r E_0^2u_0^2(1+u_0^2)^{-3}\ell^{-1}(N_a q)^{-1}$, where k_B is the Boltzman constant, q is the electron charge, and N_a is the crystal acceptor impurity concentration. In turn, the numerical analysis of the electric field problem, two results of which are shown in Figs. 2(a) and 2(b), for a given circular-symmetric intensity profile I with a transverse size ℓ, indicates that $E_a\propto E_0$ (see also Ref. 19). For example, in the cases of Figs. 2(a) and 2(b), $E_a=\alpha E_0$, with $\alpha\simeq 0.05$ for both

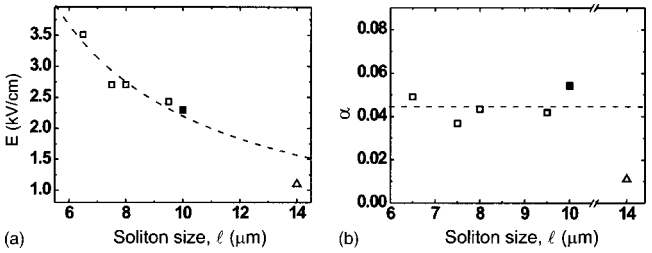

FIG. 3. Comparison between the experimental round soliton existence points (squares) and the predicted scaling for (a) condition (i) and (b) condition (ii). The filled square refers to the observation reported in Ref. 21. The triangle refers to conditions of Fig. 1(d), leading to an *elliptical* beam shape.

$\ell_0 = 6.5$ and 14 μm (note that in the first case the remaining lobe is doubled by the nonlocal components). If condition (ii) is sound, this implies that for all conditions leading to round solitons, E_n/E_a must remain constant. In other terms, $(E_d+E_s)/E_0 \approx \alpha$. Note that this implicates, in general, material parameters as well, such as the values of N_a and ϵ_r.

To test the lobe suppression mechanism described above, we analyzed a set of round soliton-supporting conditions. The study refers to values of u_0 ranging from 1.4 to 2.4, which, in terms of condition (i), involves the region of transition from unsaturated-to-saturated self-trapping, where the normalized soliton width $\Delta\xi \simeq \Delta\xi_{\min}$ is approximately independent of u_0.[10] In a centrosymmetric sample, for which the details of the local existence curve will, in general, differ from that reported in Ref. 10, this implies that $E_0 = \{\Delta\xi_{\min}/[\epsilon_0(\epsilon_r-1)kn\sqrt{g}]\}\ell^{-1}$. Experiments lead to *round* solitons, for $\ell = 6.5-10\ \mu m$, for values of E_0 versus ℓ reported in Fig. 3(a). These confirm the expected scaling, with an $(E_0\ell)_{\exp} \simeq 2.2$ V, which implies $\Delta\xi_{\min} \simeq 5.6$ (in Ref. 10, $\Delta\xi_{\min} \simeq 4$). In order to verify condition (ii), the three parameters (E_0, u_0, ℓ), of these same observations must combine to give a constant: $\alpha \approx (E_d+E_s)/E_0$. As shown in Fig. 3(b), this is the case, and forms the experimental verification of the physical picture. In order for the measured value of $\alpha_{\exp}$ to also coincide with the value estimated through the numerical approach, we must assume that $N_a \simeq 1.4\times 10^{16}$ cm^{-3} (giving $\alpha \simeq 0.045$), a value wholly compatible with those generally measured through two-wave-mixing techniques.[1] To appreciate the selectivity of the analysis, we note that the condition not leading to round self-trapping of Fig. 1(d) corresponds to a value of $\alpha \simeq 0.011$ [the triangle in Figs. 3(a) and 3(b)].

The lobe-suppression picture can be extended to describe experiments in strontium-barium-niobate (SBN)[7] and in KLTN[14] for higher values of u_0, where the simplified scaling $E_0^{1/2} \propto \ell^{-1}$ ($E_0 \propto \ell^{-1}$ for KLTN) will not hold, since $\Delta\xi$ is a function of u_0, providing a relationship between E_0, ℓ, and u_0, which does not follow from the generally reported $\Delta\xi$ versus u_0. We can, however, note that the saturation component E_s scales with ϵ_r/N_a. This means that for standard values of N_a, crystals with lower values of ϵ_r (along the optical axis), such as $BaTiO_3$ (Ref. 12) and $KNbO_3$ (Ref. 17) will have a greater difficulty in satisfying condition (ii), if compared to SBN and KLTN.

We identify the mechanism that allows round solitons in the asymmetric suppression of part of the anisotropic photorefractive response by charge diffusion and saturation effects. This implies a soliton existence curve in the three-dimensional parameter space $[E_0, \ell, u_0]$, as opposed to the reduced parameter space $[\Delta\xi = \Delta\xi(E_0, \ell), u_0]$, where E_0 and ℓ do not appear separately. This can form the key to the understanding of apparently contradictory results, and indicates the basic recipe to generate the building block of guided electro-optic devices in three-dimensional crystals.

Research was funded by the Italian Istituto Nazionale Fisica della Materia (INFM) through the "Solitons embedded in holograms" (SEH) project, and by the Italian Ministry of Research through the "Space-time effects" Basic Research FIRB project. One of the authors (E. P.) acknowledges the support of the DEWS Center for Excellence.

[1] *Spatial Solitons*, edited by S. Trillo and W. Torruellas (Springer, Berlin, 2001), Chaps. 4–5.
[2] J. Petter, C. Denz, A. Stepken, and F. Kaiser, J. Opt. Soc. Am. B **19**, 1145 (2002); J. Petter, J. Schroder, D. Trager, and C. Denz, Opt. Lett. **28**, 438 (2003).
[3] E. DelRe, B. Crosignani, P. Di Porto, E. Palange, and A. J. Agranat, Opt. Lett. **27**, 2188 (2002).
[4] S. Lan, C. Anastassiou, M. Segev, M. Shih, J. A. Giordmaine, and G. Mizell, Appl. Phys. Lett. **77**, 2101 (2000); C. B. Lou, J. J. Xu, H. J. Qiao, X. Z. Zhang, Y. L. Chen, and Z. Chen, Opt. Lett. **29**, 953 (2004).
[5] M. F. Shih, M. Segev, G. C. Valley, G. Salamo, B. Crosignani, and P. Di Porto, Electron. Lett. **31**, 826 (1995)
[6] E. DelRe, E. Palange, and A. J. Agranat, J. Appl. Phys. **95**, 3822 (2004); A. D'Ercole, E. Palange, E. DelRe, A. Ciattoni, B. Crosignani, and A. J. Agranat, Appl. Phys. Lett. **85**, 2679 (2004).
[7] M. Shih, P. Leach, M. Segev, M. Garrett, G. Salamo, and G. C. Valley, Opt. Lett. **21**, 324 (1996).
[8] A. A. Zozulya and D. Z. Anderson, Europhys. Lett. **36**, 419 (1996).
[9] S. Gatz and J. Herrmann, Opt. Lett. **23**, 1176 (1998).
[10] B. Crosignani, P. DiPorto, A. Degasperis, M. Segev, and S. Trillo, J. Opt. Soc. Am. B **14**, 3078 (1997).
[11] M. Saffman and A. A. Zozulya, Opt. Lett. **23**, 1579 (1998).
[12] J. A. Andrade-Lucio, M. D. Iturbe-Castillo, P. A. Marquez-Aguilar, and R. Ramos-Garcia, Opt. Quantum Electron. **30**, 829 (1998).
[13] G. C. Duree, J. L. Shultz, G. J. Salamo, M. Segev, A. Yariv, B. Crosignani, P. Di Porto, E. J. Sharp, and R. R. Neurgaonkar, Phys. Rev. Lett. **71**, 533 (1993).
[14] E. DelRe, M. Tamburrini, M. Segev, E. Refaeli, and A. J. Agranat, Appl. Phys. Lett. **73**, 16 (1998).
[15] H. X. Meng, G. Salamo, and M. Segev, Opt. Lett. **23**, 897 (1998).
[16] W. Krolikowski, M. Saffman, B. Luther-Davies, and C. Denz, Phys. Rev. Lett. **80**, 3240 (1998).
[17] S. Lan, M. F. Shih, and M. Segev, Opt. Lett. **22**, 1467 (1997).
[18] S. Gatz and J. Herrmann, J. Opt. Soc. Am. B **14**, 1795 (1997).
[19] N. Korneev, P. A. Marquez-Aguilar, J. J. Sanchez-Mondragon, and S. Stepanov, J. Mod. Opt. **43**, 311 (1996).
[20] A. A. Zozulya and D. Z. Anderson, Phys. Rev. A **51**, 1520 (1995).
[21] E. DelRe, A. Ciattoni, and A. J. Agranat, Opt. Lett. **26**, 908 (2001).
[22] S. R. Singh, M. I. Carvalho, and D. N. Christodoulides, Opt. Commun. **130**, 288 (1996).